The role of coronary CT angiography in advanced pericoronary adipose tissue analysis and planning of atrial fibrillation ablation procedure

Ph.D. thesis

Melinda Boussoussou M.D.

Doctoral School of Theoretical and Translational Medicine

Supervisors: Prof. Dr. Pál Maurovich-Horvat M.D. D.Sc

Dr. Bálint Szilveszter M.D. Ph.D.

Official reviewers: Dr. Viktor Kolozsvári Rudolf M.D. Ph.D.

Dr. Zsigmond Máté Jenei M.D. Ph.D.

Head of the Complex Examination Committee:

Prof. Dr. István Karádi M.D. D.Sc

Members of the Complex Examination Committee:

Prof. Dr. Henriette Farkas M.D. D.Sc

Dr. Hassan Charaf D.Sc

Budapest
2023

1 INTRODUCTION

1.1 Pericoronary adipose tissue analysis

As a biomarker for coronary inflammation pericoronary adipose tissue (PCAT) detection by coronary CT angiography (CTA) has been recently identified as a surrogate measure to independently predict plaque progression and cardiac mortality as it can detect the changes in the size of adipocytes and the accumulation of lipids through CT attenuation values. These changes are represented in increased Hounsfield unit (HU) values of PCAT on CCTA scans, called PCAT markers (PCAT attenuation and gradient). Previously reported changes between PCAT markers and patient groups are subtle and could be affected by patient and image acquisition parameters.

On the other hand, coronary calcium-score is a well-established risk marker for the identification of major adverse cardiovascular events (MACE). Therefore, patients with zero calcium-score might be suitable for analyzing a low cardiovascular-risk patient population. However, even among this patient population, the prevalence and progression of non-calcified plaque (NCP) are noticeable and NCPs are considered more vulnerable than calcified plaques with a stronger prediction for MACE. Hence it is reasonable to analyze PCAT markers in a zero calcium-score patient population to firstly identify the normal range of PCAT attenuation and to evaluate its association with NCP.

1.2 Left atrial wall thickness and pulmonary vein analysis

Atrial fibrillation (AF) is considered the most common sustained cardiac arrhythmia. Pulmonary vein isolation (PVI) became the cornerstone AF treatment as triggers of AF originate from the pulmonary veins (PVs). One of the latest catheter ablation strategies is the CLOSE protocol, a contact-force-guided approach with the use of optimized and contiguous radiofrequency lesions for the enclosure of pulmonary veins. Undoubtedly, CCTA has an important role in AF ablation, as it guides the optimal patient selection and helps in the planning of the procedure. Information about CCTA assessed left atrial wall thickness (LAWT) and PV anatomy, may alter the efficacy of radiofrequency catheter ablation. It has been hypothesized that larger local atrial wall thickness might lead to the

reconnection of PVs, hence the CLOSE protocol may need further adjustments to create appropriate LA lesions. We hypothesized that using the novel modified CLOSE protocol appropriate isolation of the PVs is feasible regardless of patient LAWT. First-pass isolation is an invaluable indicator of acute procedural success of PVI thus the effectiveness of the ablation protocol used. The effect of LAWT and PV anatomy on successful first-pass isolation has not yet been evaluated. Hence our study aim was to define the relationship between CCTA-derived LAWT and PV measurements and the acute procedural success of the modified CLOSE protocol assessed by first-pass isolation.

2 OBJECTIVES

2.1 Pericoronary adipose tissue analysis

- To evaluate the associations between NCP markers and PCAT attenuation and gradient in patients with a low cardiovascular risk (calcium scores =0).
- To evaluate to what degree patient and imaging characteristics influence PCAT markers.
- To assess whether potential associations between NCP and PCAT markers persisted after correcting for patient and imaging characteristics.
- To validate our findings in a cohort of individuals with zero calcium scores but imaged using a different CT scanner, and on a group of patients with moderate to severe stenosis on CCTA.

2.2 Left atrial wall thickness and pulmonary vein analysis

- To determine the relationship between the acute procedural success of CLOSE protocol and LAWT.
- To evaluate the potential role of PV anatomy in the rate of first-pass isolation.

3 METHODS

3.1 Pericoronary adipose tissue analysis

3.1.1 Patient population and validation groups

In our retrospective, observational, single-centre study, 1652 consecutive patients had CCTA examination between April 2016 and August 2019 for stable chest pain evaluation and had a calcium score of zero, as an indicator of a low cardiovascular risk patient population. The inclusion criteria of the study were the following: 1) proper image quality of the patients for PCAT analysis and 2) the absence of calcium on non-contrast CT images. Exclusion criteria were 1) images not available from the PACS system 2) poor image quality 3) tube voltage other than 100 or 120 kVp 4) prior CAD of the patients.

We retrospectively identified two additional validation groups, 330-330 patients in each group to validate our finding (20-20 % of the Zero calcium score group). The Zero calcium-score group (n=330) with a different scanner was the first validation group with the same inclusion and exclusion criteria as the primary group. The Moderate to severe CAD group (n=330) represented the second validation group comprised of individuals scanned on the same scanner as the primary study group.

3.1.2 Sensitivity analysis

To assess whether our results regarding the link between patient and image acquisition parameters and PCAT markers are valid in patients without any CAD, we carried out a sensitivity analysis in patients from our primary study group with zero calcium score and no NCP.

3.1.3 Coronary CTA acquisition

Imaging was performed with a 256-slice scanner (Brilliance iCT 256, Philips Healthcare) on individuals that were in the Zero calcium score group and the Moderate to severe CAD validation group, whereas the Zero calcium score group -different scanner validation group consisted of patients with images done by a dedicated cardiac CT scanner (CardioGraphe, GE Healthcare). Both scanners used prospective ECG-triggering in axial acquisition mode.

3.1.4 Coronary CTA plaque characterization

Segment stenosis was defined by summing the stenosis score of each segment and classified as the following: (0) none (0%); (1) minimal (1–24%); (2) mild (25–49%); (3) moderate (50–69%), (4) severe (70–99%) or (5) occluded (100%). Obstructive stenosis was defined as equal to or more than 50% of the diameter stenosis. Segment involvement score was estimated by the summation of every segment score. In the case of no plaque, the score was zero in the given segment, while a score of one was determined when a plaque or plaques were present in the given segment. Both scores were continuous variables and were included in the statistical models. High-risk plaque features were determined as positive remodeling, low-attenuation plaque, spotty calcification and napkin-ring sign based on standardized definition. High-risk plaque was defined when two of the abovementioned features were present.

3.1.5 Image quality analysis

Contrast-to-noise ratio (CNR) and signal-to-noise ratio (SNR) were calculated by manually placing a circular region of interest in the pericoronary adipose tissue (PCAT), around the proximal right coronary artery, in the aorta and in the right coronary artery to attain mean CT numbers in Hounsfield Units (HU). Motion artifacts and regions that were inhomogeneous were avoided. As our interest was the location of the PCAT measurements CNR and SNR were calculated based on the CT attenuation of the aortic root at the level of the ostium of the RCA. The definition of the CNR: CNR= (RCA HU-PCAT HU)/Aorta standard deviation, while SNR= RCA HU/Aorta standard deviation. The measurements were blinded to all PCAT and clinical data.

3.1.6 Pericoronary adipose tissue analysis

The proximal segment of the RCA was the location where PCAT analysis was carried out using the AutoPlaque software (version 2.0, Cedars-Sinai Medical Center), (Figure 1.) in the 40 mm proximal RCA segment, excluding the first 10 mm segment from the ostium. Voxels between -190 HU and -30 HU are defined as adipose tissue, therefore all PCAT markers were assessed after removing all voxels with values above or below this range. PCAT

attenuation was determined as the average HU attenuation within a radial distance from the outer coronary artery wall equal to the average diameter of the vessel. PCAT gradient was calculated as the percentage change in PCAT attenuation when comparing PCAT HU values to non-PCAT HU values, (100%*(PCAT attenuation - non-PCAT attenuation)/|PCAT attenuation|).

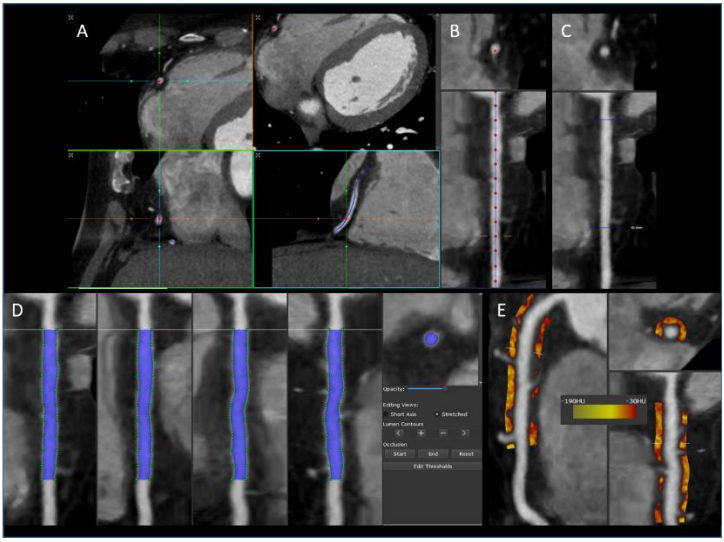

Figure 1. PCAT analysis by the AutoPlaque software step by step.

Panel **A** shows the first step of PCAT analysis. The RCA segment is chosen by marking the proximal (RCA ostium) and the distal part of the RCA. Panel **B** displays the step when the RCA centreline is corrected point by point if necessary. Panel **C** shows the standardized model with a 40 mm segment marked 10 mm distal from the RCA ostium. This 40 mm segment is depicted in panel **D** where the blue areas represent the RCA's lumen in four different angles in a sagittal view and one in an axial view. After the necessary corrections, the AutoPlaque software calculates the PCAT around the given 40 mm segment (Panel **E**). The shades of orange represent the HU unit values

within the range of -190 HU to - 30 HU in the two sagittal planes as well as in the axial plane.

Abbreviation: RCA: right coronary artery, PCAT: pericoronary adipose tissue

3.1.7 Cardiovascular outcome analysis

In every study group, the patients were followed up using the Hungarian Myocardial Infarction Registry to screen if they experienced an acute myocardial infarction after the CCTA examination.

3.1.8 Statistical analysis

Analyses were calculated in R environment (v4.0.2). Categorical parameters are presented as frequency (percentages), while continuous variables are represented as mean (standard deviation). A linear regression model was used to analyze clinical, imaging and CAD predictors of PCAT markers. Multivariable models were built comprising all predictors into the regression model. A $p < 0.05$ was considered significant.

3.2 Left atrial wall thickness and pulmonary vein analysis

3.2.1 Patient population

In our prospective, observational single-centre cohort study, 186 consecutive patients were screened who had symptomatic drug-refractory AF and received radiofrequency catheter ablation from January 2019 to September 2020. Exclusion criteria were the following: 1) prior catheter ablation procedure 2) no pre-procedural CCTA was done 3) poor CCTA image quality. Overall, 94 patients' scans were analysed.

3.2.2 Imaging of the left atrium and pulmonary veins with coronary CTA

In the study population, every patient had contrast-enhanced prospective ECG-triggered CCTA (256-slice scanner Brilliance iCT 256, Philips Healthcare, Best, The Netherlands) prior to the catheter ablation procedure.

3.2.3 Image analysis

Commercially available Philips IntelliSpace Portal v.6.2, (Philips Healthcare) software was used for the measurement of LAWT and PVs. Eleven separate LA locations were chosen for the assessment of the maximum wall thickness areas (right, middle and left regions of the atrium and mid-posterior and infero-posterior areas) (Figure 2.).

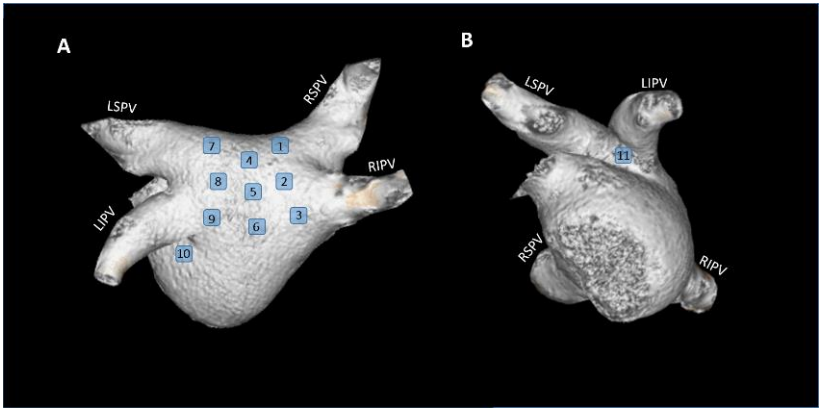

Figure 2. Volume-rendered 3D CCTA images demonstrate the 11 locations where LAWT was measured in the left atrium.

On panel **A** the LA is in a posterior view while panel **B** displays the left lateral view of the LA. The numbers represent the following left atrial areas: 1: right roof, 2: right mid-posterior, 3: right infero-posterior, 4: middle part of the roof, 5: middle part of the mid-posterior, 6: middle part of the infero-posterior, 7: left of the roof, 8: left of the mid-posterior, 9: left of the infero-posterior, 10: mitral isthmus, 11: left lateral ridge.

Abbreviations: 3D: three-dimensional, CCTA: coronary computed tomography angiography, LA: left atrium, LAWT: left atrial wall thickness, LIPV: left inferior pulmonary vein, LSPV: left superior pulmonary vein, RIPV: right inferior pulmonary vein, RSPV: right superior pulmonary vein.

The anatomy and diameter of the PVs were also evaluated in this patient population. A PV anatomy was considered normal when at both sides of the

LA two-two distinct pulmonary veins were present (right superior and inferior and left superior and inferior).

3.2.4 Pulmonary vein isolation procedure

PVI was carried out using the CARTO3 electroanatomical mapping system. with radiofrequency energy using the point-by-point technique. The aim of every procedure was to reach electrical isolation of all PVs from the LA with contiguous and circumferential lines of ablation. Firstly, with a multipolar mapping catheter, a fast anatomical map from the LA was generated. Secondly, using the ThermoCool SmartTouch® ablation catheter and a steerable sheath, radiofrequency ablations were applied in a point-by-point manner. The modified CLOSE protocol was used to guide the ablations: ablation index (AI) target value was 500 on the anterior and 400 on the posterior wall, inter-lesion distance at all sites was < 6 mm, and target contact force 10-40 g. After finishing the circumferential ablation line around the given PV, in order to evaluate entrance and exit blocks, hence the acute success of the PVI, the mapping catheter was placed in the vein. When local PV potentials were absent on the mapping catheter, the entrance block was confirmed, whereas the exit block was assessed by pacing at several sites inside the PVs. When both entrance and exit block was present first-pass isolation was stated. The absence of first-pass isolation was defined by the persistence of PV conduction. In such cases, the ablation was continued until both entrance and exit block was achieved. After an ablation site was finished the mapping catheter was left in those PVs and the ablation was continued at the other sides. In order to assess acute PV reconnection, each PV was evaluated repeatedly after 20 minutes. In uncomplicated cases, patients were discharged the day after the procedure.

3.2.5 Statistical analysis

Each analysis was conducted by STATA v13.0. Categorical parameters are presented as frequency (percentages), while continuous variables are represented as mean (standard deviation). For the comparison of LAWT and different LA wall territories or for the assessment of the differences between PVs with the absence or presence of first-pass isolation, independent sample

t-test was used. After that, in order to identify predictors of procedural success of right or left PVs, logistic regression was applied. To evaluate the reproducibility of the measurements including intra- and inter-observer agreement intraclass correlation coefficient (ICC) was used in 20 patients by a single reader. A two-sided p-value less than 0.05 was considered statistically significant.

4 RESULTS

4.1 Pericoronary adipose tissue analysis

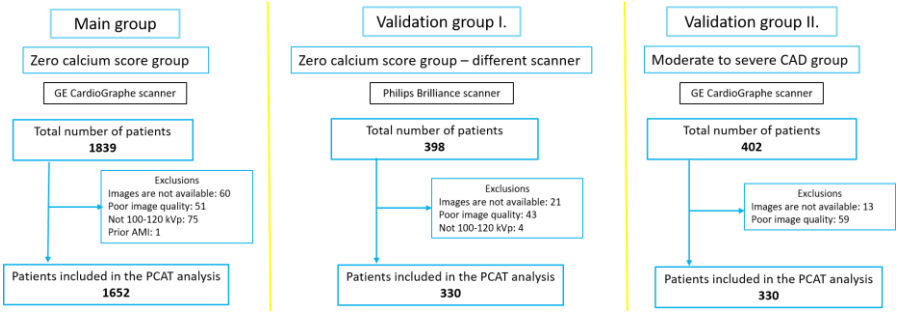

Figure 3. Study design. (Own work.)
Study design of the Main group and the two Validation groups.
Abbreviations: AMI: acute myocardial infarction, CAD: coronary artery disease, kVp: kilovoltage peak, PCAT: pericoronary adipose tissue

4.1.1 Patient characteristics

4.1.1.1 Zero calcium score group

For the assessment of stable chest pain, 4120 consecutive patients underwent CCTA examination between 2016 and 2019. Among this patient population 1839 patients had a zero calcium score. The number of patients excluded from the analysis was 187. Overall, 1652 patients were analysed in the Zero calcium score group who met all the inclusion and exclusion criteria. The mean age of the patients was 51±11 years, and 871 patients (53%) were female. Overall, 649 (39%) individuals had plaques.

4.1.1.2 Zero calcium score group – different scanner

Overall, to have the 20% of the number of Zero calcium score group 398 images were analysed to have 330 scans suitable for PCAT measurements.

4.1.1.3 Moderate to severe CAD group

Overall, 402 scans were screened to achieve 330 scans suitable for PCAT measurements

4.1.2 Predictors of PCAT attenuation in the Zero calcium score group

In individuals with zero calcium score, the range between PCAT values was -123 HU and -51 HU. Average PCAT attenuation was -92 ± 9 HU, whereas the median value was: -93 HU (25th percentile: -99 HU; 75th percentile: -87 HU).

4.1.2.1 Univariable analysis

Among CAD characteristics, the presence of NCP, segment stenosis score (SSS), segment involvement score (SIS) and high-risk plaque were associated with an increasing PCAT attenuation (2, 1, 1, 6 HU respectively; $p<0.001$ for all), whereas there was no evidence of an association between PCAT attenuation and the presence of obstructive stenosis (1HU, p=0.58).

4.1.2.2 Multivariable analysis

In the multivariable analysis, among the clinical characteristics of the patients and their image acquisition parameters, male sex, 120 kVp instead of 100 kVp, signal-to-noise ratio and pixel spacing were independently associated with higher PCAT attenuation values (1 HU p=0.003, 8 HU $p<0.001$, 1 HU $p<0.001$, 32 HU $p<0.001$; respectively). While the followings decreased independently PCAT attenuation: each kg/m^2 increase in body mass index, beat/minute in heart rate, mAs in tube current, unit in contrast to noise ratio (-0.4 HU, -0.2 HU, -0.02 HU, -1.3 HU; $p<0.001$ for all; respectively). Moreover, none of the CAD characteristics was associated with PCAT attenuation (presence of NCP (0 HU, p=0.93) presence of obstructive stenosis (1 HU, p=0.71), SSS (0 HU, p=0.39), SIS (1 HU,

p=0.18), high-risk plaque (2 HU, p=0.10)). Detailed results are shown in Table 1.

Table 1. The relationship between clinical characteristics, CCTA acquisition parameters, coronary artery disease characteristics and PCAT attenuation in the Zero calcium score study groups.

Predictors	Zero calcium score group (n=1652)					
	Univariable model			Multivariable model		
	HU	95% CI	p	HU	95% CI	p
Clinical characteristics						
Age [y]	0.1	[0.0; 0.1]	**0.001**	0.0	[-0.1; 0.0]	0.23
Male sex	2.6	[1.7; 3.5]	**<0.001**	1.4	[0.5; 2.3]	**0.003**
BMI [kg/m^2]	0.1	[0.0; 0.2]	0.14	-0.4	[-0.5; -0.3]	**<0.001**
Hypertension [mmHg]	1.1	[0.2; 2.0]	**0.01**	0.3	[-0.6; 1.1]	0.53
Diabetes	0.7	[-1.1; 2.4]	0.46	0.7	[-1.0; 2.3]	0.42
Dyslipidemia	0.5	[-0.5; 1.5]	0.30	0.1	[-0.8; 1.0]	0.88
Smoking	0.3	[-0.9; 1.6]	0.62	0.1	[-1.0; 1.2]	0.92
CCTA acquisition parameters						
Non-sinus rhythm	1.3	[-1.9; 4.4]	0.44	2.6	[-0.3; 5.5]	0.08
Heart rate [beats/minute]	-0.2	[-0.3; -0.2]	**<0.001**	-0.2	[-0.2; -0.1]	**<0.001**
Poor image quality	-3.6	[-5.4; -1.8]	**<0.001**	-1.3	[-3.0; 0.5]	0.15
Tube voltage 120 kVp	6.2	[5.4; 7.1]	**<0.001**	7.7	[6.7; 8.7]	**<0.001**
Tube current [mAs]	-0.02	[-0.03; -0.004]	**0.01**	-0.02	[-0.03; -0.01]	**<0.001**
CNR	0.0	[-0.1; 0.1]	0.94	-1.3	[-1.7; -1.0]	**<0.001**
SNR	0.0	[0.0; 0.1]	0.48	1.4	[1.0; 1.7]	**<0.001**
Pixel Spacing [mm^3]	30.5	[22.5; 38.6]	**<0.001**	32.4	[24.9; 39.9]	**<0.001**
Coronary artery disease characteristics						
Presence of plaque	2.3	[1.4; 3.3]	**<0.001**	0.1	[-1.2; 1.4]	0.93
Presence of obstructive stenosis	1.3	[-3.4; 6.1]	0.58	1.1	[-4.5; 6.6]	0.71
SSS [n]	0.6	[0.3; 0.8]	**<0.001**	-0.4	[-1.1; 0.4]	0.39
SIS [n]	1.0	[0.6; 1.4]	**<0.001**	0.8	[-0.4; 2.0]	0.18
Presence of HRP	5.6	[3.2; 8.1]	**<0.001**	1.9	[-0.3; 4.2]	0.10

Univariable and multivariable linear regression models demonstrating the effects of clinical characteristics, CTA acquisition setting and CAD characteristics on PCAT attenuation. Significant predictors are marked in bold. All variables were entered into the multivariable models. *Abbreviations: BMI: body mass index, CAD: coronary artery disease, CNR: contrast to noise ratio, CTA: coronary CT angiography, HRP: High-risk*

plaque, kVp: kilovoltage peak, mAs: milliampere-second, PCAT: pericoronary adipose tissue, SIS: Segment involvement score, SNR: Signal to noise ratio, SSS: Segment Stenosis Score.

4.1.3 Predictors of PCAT gradient in the Zero calcium score group

The range between the PCAT gradient values was -31% to 75% in patients with zero calcium score. The average PCAT gradient value among individuals with a calcium score of zero was: -1±12%, whereas the median value was: -2% (25th percentile: -9%; 75th percentile: 6%).

4.1.3.1 Univariable analysis

A significant association was found between all CAD parameters and PCAT gradient: the presence of NCP (-2% p<0.001), presence of obstructive stenosis (8% p=.01), SSS (1% p<0.001), SIS (1% p<0.001), high-risk plaque (5% p<0.001).

4.1.3.2 Multivariable analysis

In the multivariable analysis after correcting for all factors, age (0.1% p<0.001), male sex (3% p<0.001), non-sinus rhythm (6% p=0.01), 120 kVp (4% p<.001) SNR (1% p<.001), and pixel spacing (37% p<0.001) were all independently associated with higher PCAT gradient values. Contrarily, each beat per minute increase in heart rate (-0.1% p=0.02), each increase in mAs (-0.02% p=.003) and CNR (-1% p<0.001) was independently associated with lower PCAT gradient values. Moreover, none of the CAD characteristics showed evidence of an association with PCAT gradient: presence of NCP (0% p=0.79), presence of obstructive stenosis (4% p=0.28), SSS (0% p=0.94) SIS (0% p=0.65) and presence of high-risk plaque (2% p=0.25).

Similar results were found in the validation groups. After correcting for patient and image acquisition parameters the univariate association between the CAD characteristics and PCAT markers disappeared, while several of the patient and image acquisition parameters remained significantly associated with PCAT markers.

4.1.4 Cardiovascular outcome analysis

In the Zero calcium score group, during the average 3.0 years follow-up time, two patients had AMI, with PCAT attenuation and gradient values of -93HU

and -79 HU and -1% and 19% respectively. In the Zero calcium score - different scanner validation cohort, no events occurred within the average follow-up time of 0.7 years, whereas there were 7 events with an average of 2.2 years in the Moderate to severe CAD group. The PCAT attenuation ranged between -88 HU and -64 HU, while the gradient values were between 7% to 51%.

Representative images from all three groups showing how different heart rates influence PCAT attenuation and PCAT gradient values are shown in Figure 4.

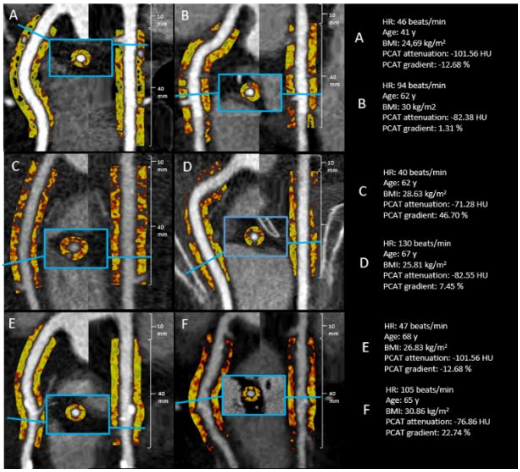

Figure 4. Representative images showing PCAT attenuation and PCAT gradient differences in patients with different heart rates.

Panels **A** and **B** show two representative images from the Zero calcium score group. Patients were scanned on a Philips - Brilliance iCT 256 and had a calcium score of zero. Panels **C** and **D** show two representative cases from the Zero calcium score - different scanner group. Patients were scanned on a GE - CardioGraphe and had a calcium score of zero. Panels **E** and **F** show two representative images from the Moderate to severe CAD group. Patients were scanned on a Philips - Brilliance iCT 256 and had obstructive CAD. Patients within all three cohorts had a wide range of PCAT attenuation and gradient values.

Abbreviations: BMI: body mass index, CAD: coronary artery disease, HR: heart rate, HU: Hounsfield unit, PCAT: pericoronary adipose tissue.

4.1 Left atrial wall thickness and pulmonary vein analysis

4.1.1 Patient characteristics

Overall, 94 patients were included in the analysis. The mean age was 62.4±12.6 years, mean BMI 28.1±3.5 kg/m^2, 39.4% female. A total of 1034 LAWT were measured and 376 PV ostium diameters and areas were analysed.

4.1.2 Left atrial measurement

The mean LAWT value was 1.35±0.46 with a range of 0.2-2.6 mm. Regional differences were assessed by combining several measurement points. We found that LAWT on the right side (roof, mid-posterior, infero-posterior) was significantly larger as compared to the middle (roof, mid-posterior, infero-posterior) and left side (roof, mid-posterior, infero-posterior) (all $p<0.01$). The infero-posterior region (right infero-posterior, middle infero-posterior, left infero-posterior) was substantially thinner than the mean middle (right mid-posterior, middle mid-posterior, left mid-posterior) and mean roof total (right roof, middle roof, left roof ($p=0.01$ and $p=0.08$, respectively).

4.1.3 The effect of clinical and CT-derived parameters on the first-pass isolation rate

In 100% of the PVs, complete electrical isolation of all PVs was achieved. There were no periprocedural complications. Successful first-pass isolation was achieved in 71 cases on the left side and 67 cases on the right side. Successful first-pass isolation of all PVs was achieved in 51 patients. There were no acute reconnections during the 20 min waiting period after the ablation. Regarding anthropometrics and clinical risk factors, we detected no association with the first-pass isolation success rate, based on univariate regression analysis, regardless of left, right or both-sided first-pass isolation. Shorter procedural time was found in those cases, where first-pass isolation was achieved on both sides ($p=0.03$).

We also found that LAWT did not influence the first-pass isolation rate during PVI guided by our standardized ablation strategy.

Among all assessed parameters, only the diameter of the RSPV was associated with the success rate of right-sided first-pass isolation, as a wider RSPV diameter led to easier first-pass isolation (OR 1.01, p=0.04). Other cardiac CT and echocardiography-derived parameters did not influence the success rate of first-pass isolation (p>0.05)

Reproducibility was assessed in 20 patients at 11 regions of interest (20×11 measurements) in terms of wall thickness, moreover, the area and diameter of each pulmonary vein were also assessed. The intra- and inter-reader intraclass correlation coefficient (ICC) for the assessment of LAWT were 0.98 (CI 0.97–0.98) and 0.92 (CI 0.79–0.97), respectively. The intra-reader area and diameter ICC's minimum and maximum range were between 0.94 and 0.99 and 0.98–0.99 respectively while the inter–reader area and diameter ICC's minimum and maximum range were between 0.78–0.92 and 0.80–0.94, respectively.

Table 2. CCTA-based assessment of LA-PV parameters.

	First-pass on left side	**No first-pass on left side**	**p value**	**First-pass on right side**	**Unsuccessful first-pass on right side**	**p value**
PV diameter (mm), (mean ± SD						
LIPV	269.67 ± 220.16	224.11 ±116.93	0.31	NA	NA	NA
LSPV	280.98 ± 98.39	250.00 ± 94.61	0.19	NA	NA	NA
RSPV	NA	NA	NA	371.63 ± 111.26	312.52 ± 122.66	**0.04**
RIPV	NA	NA	NA	266.86 ± 88.35	241.81 ± 62.15	0.23
PV area (mm^2), (mean ± SD)						

LIPV	17.64 ± 5.89	16.43 ± 3.95	0.33	NA	NA	NA
LSPV	18.60 ± 3.14	17.19 ± 3.85	0.08	NA	NA	NA
RSPV	NA	NA	NA	21.34 ± 3.19	19.90 ± 3.71	0.09
RIPV	NA	NA	NA	18.04 ± 3.06	17.29 ± 2.61	0.31
LAWT (mm), (mean ± SD)						
Mean total	1.35 ± 0.46	1.32 ± 0.51	0.78	1.34 ± 0.46	1.32 ± 0.54	0.83
Mean roof	1.39 ± 0.59	1.21 ± 0.53	0.18	1.36 ± 0.56	1.27 ± 0.66	0.52
Mean mid-posterior	1.39 ± 0.60	1.41 ± 0.74	0.91	1.37 ± 0.65	1.45 ± 0.62	0.64
Mean infero-posterior	1.12 ± 0.52	1.09 ± 0.62	0.89	1.09 ± 0.55	1.18 ± 0.57	0.51
Mean left	1.21 ± 0.44	1.18 ± 0.49	0.74	NA	NA	NA
Mean right	NA	NA	NA	1.74 ± 0.66	1.79 ± 0.68	0.74

Abbreviations: CT: computer tomography, LAA flow: left atrial appendage flow, LA-PV: Left Atrial – Pulmonary Veins LAWT: left atrial wall thickness, LIPV: left inferior pulmonary vein, LSPV: left superior pulmonary vein, NA: not applicable, PV diameter: pulmonary vein diameter, RIPV: right inferior pulmonary vein, RSPV: right superior pulmonary vein, SD: standard deviation.

5 CONCLUSION

5.1 Pericoronary adipose tissue analysis

Based on our results, PCAT attenuation and gradient represent a wide range of values in low cardiovascular risk patient population (calcium score=0). PCAT markers are significantly influenced by different patient characteristics and image acquisition parameters. After correcting for these characteristics the association between CAD and PCAT markers disappears, highlighting the importance of correcting for all possible confounders before evaluating the additive value of PCAT markers. In order to validate the additive value of PCAT markers, extensive correction for possible cofounders is needed in future studies.

5.2 Left atrial wall thickness and pulmonary vein analysis

The usage of standardized ablation protocol in persistent and paroxysmal AF patients leads to a high first-pass isolation rate with high acute procedural success that was independent of the LAWT. In terms of RSPV, a larger diameter showed a link with right-sided successful first-pass isolation.

6 BIBLIOGRAPHY OF THE CANDIDATE

1. **Boussoussou M**, Vattay B, Szilveszter B, Simon J, Lin A, Vecsey-Nagy M, et al. The effect of patient and imaging characteristics on coronary CT angiography assessed pericoronary adipose tissue attenuation and gradient. Journal of cardiovascular computed tomography. 2023;17(1):34-42. **IF: 5,17**
2. **Boussoussou M**, Szilveszter B, Vattay B, Kolossváry M, Vecsey-Nagy M, Salló Z, et al. The effect of left atrial wall thickness and pulmonary vein sizes on the acute procedural success of atrial fibrillation ablation. Int J Cardiovasc Imaging. 2022. **IF: 2,1**

Bibliography not related to the present thesis

1. **Boussoussou M**, Édes István F, Nowotta F, Vattay B, Vecseys-Nagy M, Drobni Zs et al. Coronary CT-based FFR in patients with acute myocardial infarction might predict follow-up invasive FFR: The XPECT-MI study. Journal of cardiovascular computed tomography. 2023;17(4):269-76. **IF: 5,4**
2. Maurovich-Horvat P, Bosserdt M, Kofoed KF, Rieckmann N, Benedek T, Donnelly P, … **Boussoussou M,** et al. CT or Invasive Coronary Angiography in Stable Chest Pain. N Engl J Med. 2022;386(17):1591-602. **IF: 176,079**
3. Panajotu A, Vecsey-Nagy M, Jermendy Á L, **Boussoussou M**, Vattay B, Kolossváry M, et al. Coronary CTA Amidst the COVID-19 Pandemic: A Quicker Examination Protocol with Preserved Image Quality Using a Dedicated Cardiac Scanner. Diagnostics (Basel, Switzerland). 2023;13(3). **IF: 3,6**
4. Vattay B, Szilveszter B, **Boussoussou M**, Vecsey-Nagy M, Lin A, Konkoly G, et al. Impact of virtual monoenergetic levels on coronary plaque volume components using photon-counting computed tomography. European radiology. 2023. **IF: 5,9**
5. Vecsey-Nagy M, Varga-Szemes A, Emrich T, Zsarnoczay E, Nagy N, Fink N, … **Boussoussou M**, et al. Calcium scoring on coronary computed angiography tomography with photon-counting detector technology: Predictors of performance. Journal of cardiovascular computed tomography. 2023. **IF: 5,4**
6. Vecsey-Nagy M, Jokkel Z, Jermendy Á L, Nagy M, Boussoussou M, Vattay B, et al. The Impact of Novel Reconstruction Algorithms on Calcium Scoring:

Results on a Dedicated Cardiac CT Scanner. Diagnostics (Basel, Switzerland). 2023;13(4). **IF: 3,6**

7. Vattay B, Borzsák S, **Boussoussou M**, Vecsey-Nagy M, Jermendy Á L, Suhai FI, et al. Association between coronary plaque volume and myocardial ischemia detected by dynamic perfusion CT imaging. Front Cardiovasc Med. 2022;9:974805. **IF: 5,846**
8. Vattay B, Nagy AI, Apor A, Kolossváry M, Manouras A, Vecsey-Nagy M, … **Boussoussou M,** et al. The Predictive Value of Left Atrial Strain Following Transcatheter Aortic Valve Implantation on Anatomical and Functional Reverse Remodeling in a Multi-Modality Study. Front Cardiovasc Med. 2022;9:841658. **IF: 5,846**
9. Vecsey-Nagy M, Szilveszter B, Kolossváry M, **Boussoussou M**, Vattay B, Merkely B, et al. Correlation between Coronary Artery Calcium- and Different Cardiovascular Risk Score-Based Methods for the Estimation of Vascular Age in Caucasian Patients. J Clin Med. 2022;11(4). **IF: 4,964**
10. Vecsey-Nagy M, Szilveszter B, Kolossváry M, **Boussoussou M**, Vattay B, Gonda X, et al. Cyclothymic affective temperament is independently associated with left ventricular hypertrophy in chronic hypertensive patients. J Psychosom Res. 2022;160:110988. **IF: 4,620**
11. Vecsey-Nagy M, Jermendy Á L, Kolossváry M, Vattay B, **Boussoussou M**, Suhai FI, et al. Heart Rate-Dependent Degree of Motion Artifacts in Coronary CT Angiography Acquired by a Novel Purpose-Built Cardiac CT Scanner. J Clin Med. 2022;11(15). **IF: 4,964**
12. Papp S, Bárczi G, Karády J, Kolossváry M, Drobni ZD, Simon J, … **Boussoussou M,** et al. Coronary plaque burden of the left anterior descending artery in patients with or without myocardial bridge: A case-control study based on coronary CT-angiography. Int J Cardiol. 2021;327:231-5. **IF: 4,039**
13. Szilveszter B, Vattay B, **Bossoussou M**, Vecsey-Nagy M, Simon J, Merkely B, et al. CAD-RADS may underestimate coronary plaque progression as detected by serial CT angiography. Eur Heart J Cardiovasc Imaging. 2022;23(11):1530-9. **IF: 9,13**
14. Vecsey-Nagy M, Szilveszter B, Kolossváry M, **Boussoussou M**, Vattay B, Gonda X, et al. Association between affective temperaments and severe coronary artery disease. J Affect Disord. 2021;295:914-9. **IF: 6,533**
15. Vecsey-Nagy M, Jermendy Á L, Suhai FI, Panajotu A, Csőre J, Borzsák S, … **Boussoussou M,** et al. Model-based adaptive filter for a dedicated

cardiovascular CT scanner: Assessment of image noise, sharpness and quality. Eur J Radiol. 2021;145:110032. **IF: 4,531**

16. Vecsey-Nagy M, Szilveszter B, Kolossváry M, **Boussoussou M**, Vattay B, Gonda X, et al. The association between accelerated vascular aging and cyclothymic affective temperament in women. J Psychosom Res. 2021;145:110423. **IF: 4,620**
17. **Boussoussou M**, Boussoussou N, Merész G, Rakovics M, Entz L, Nemes A. Atmospheric fronts as minor cardiovascular risk factors, a new approach to preventive cardiology. J Cardiol. 2020;75(2):196-202. **IF: 3,159**
18. Simon J, Száraz L, Szilveszter B, Panajotu A, Jermendy Á, Bartykowszki A, et al. Calcium scoring: a personalized probability assessment predicts the need for additional or alternative testing to coronary CT angiography. Eur Radiol. 2020;30(10):5499-506. **IF: 5,315**
19. Boussoussou N, **Boussoussou M**, Merész G, Rakovics M, Entz L, Nemes A. Complex effects of atmospheric parameters on acute cardiovascular diseases and major cardiovascular risk factors: data from the Cardiometeorology(SM) study. Sci Rep. 2019;9(1):6358. **IF: 3,988**

Hungarian journal articles:

1. **Boussoussou M**, Vattay B, Szilveszter B, Kolossváry M, Simon J, Vecsey-Nagy M, et al. Functional assessment of coronary plaques using CT based hemodynamic simulations: Current status, technical principles and clinical value. Imaging. 2021;13(1):37-48.
2. Vattay B, **Boussoussou M**, Borzsák S, Vecsey-Nagy M, Simon J, Kolossváry M, et al. Myocardial perfusion imaging using computed tomography: Current status, clinical value and prognostic implications. Imaging. 2021;13(1):49-60.
3. Boussoussou N, Boussoussou M, Nemes A. Historical overview of medical meteorology - the new horizon in medical prevention. Orv Hetil. 2017;158(5):187-91. IF: 0,322
4. Boussoussou N, **Boussoussou M**, Entz L. Akut cardiovascularis kórképek vizsgálata különböző légköri paraméterek tükrében. Orv Hetil. 2014;155(27): 1078-1082. IF: 0,322
5. Simon J, Herczeg S, Borzsák S, Csőre J, Kardos AS, Mérges G, … **Boussoussou M**, et al. Extracardiac findings on cardiac computed tomography in patients undergoing atrial fibrillation catheter ablation. Imaging. 2022;14(1):52-9.